Materials Science & Engineering A 636 (2015) 529–535

Contents lists available at ScienceDirect

Materials Science & Engineering A

journal homepage: www.elsevier.com/locate/msea

# Creep lifing methodologies applied to a single crystal superalloy by use of small scale test techniques

S.P. Jeffs [a,*], R.J. Lancaster [a], T.E. Garcia [b]

[a] Institute of Structural Materials, Swansea University, Singleton Park SA2 8PP, United Kingdom
[b] IUTA (University Institute of Industrial Technology of Asturias), University of Oviedo, Edificio Departamental Oeste 7.1.17, Campus Universitario, 33203 Gijón, Spain

ARTICLE INFO

*Article history:*
Received 24 February 2015
Received in revised form
26 March 2015
Accepted 26 March 2015
Available online 8 April 2015

*Keywords:*
Wilshire equations
Creep
Small punch
Single crystal

ABSTRACT

In recent years, advances in creep data interpretation have been achieved either by modified Monkman–Grant relationships or through the more contemporary Wilshire equations, which offer the opportunity of predicting long term behaviour extrapolated from short term results. Long term lifing techniques prove extremely useful in creep dominated applications, such as in the power generation industry and in particular nuclear where large static loads are applied, equally a reduction in lead time for new alloy implementation within the industry is critical. The latter requirement brings about the utilisation of the small punch (SP) creep test, a widely recognised approach for obtaining useful mechanical property information from limited material volumes, as is typically the case with novel alloy development and for any in-situ mechanical testing that may be required. The ability to correlate SP creep results with uniaxial data is vital when considering the benefits of the technique. As such an equation has been developed, known as the $k_{SP}$ method, which has been proven to be an effective tool across several material systems. The current work now explores the application of the aforementioned empirical approaches to correlate small punch creep data obtained on a single crystal superalloy over a range of elevated temperatures. Finite element modelling through ABAQUS software based on the uniaxial creep data has also been implemented to characterise the SP deformation and help corroborate the experimental results.



## 1. Introduction

The small punch (SP) test method was initially developed by the nuclear industry in the 1980s to estimate the residual life of components subjected to hostile in-service environments [1]. Since then, the approach has been adopted by many other industrial sectors due to the numerous benefits that the test can offer [2,3]. Indeed, many of the advantages of this approach relates to the small volume of test material typically required and the significant cost savings that it can potentially offer, whilst producing important creep and fracture data on the respective material. The techniques have now been further developed across world-wide laboratories to obtain creep rupture and tensile fracture data over a range of material systems including steels, titanium, aluminium alloys and has been successful employed on single crystal nickel alloy systems [4–8]. Furthermore, published literature has shown how SP testing can be utilised as an effective tool for ranking creep properties of novel alloy variants in comparison to more traditional uniaxial approaches and also components fabricated through advanced manufacturing processes [8–10]. Extensive use of the SP technique has led to the publication of a European Code of Practice (CoP) in order to standardise SP testing and its application [4]. In addition, the SP CoP also proposes a SP creep correlation factor, $k_{SP}$ where the SP load can be correlated to a uniaxial creep stress in order to compare SP and conventional creep data (Eq.(1)), an approach which has been successfully applied to several material systems [5,6,11].

$$\frac{F}{\sigma} = 3.33 k_{SP} R^{-0.2} r^{1.2} h_0 \tag{1}$$

The Monkman–Grant relationship is a widely recognised technique for correlating time to rupture to minimum creep rates for uniaxial creep results [12], or in the case of SP testing, a minimum displacement or deflection rate [13]. The significance of such a relationship is that with a limited number of uniaxial or SP creep tests, the time to rupture of a long term test may be estimated. Within this work, it has been attempted to establish a formula for re-calculating the minimum

* Corresponding author. Tel.: +44 1792602061; fax: +44 1792295693.
*E-mail address:* s.p.jeffs@swansea.ac.uk (S.P. Jeffs).

http://dx.doi.org/10.1016/j.msea.2015.03.119

creep rate from the minimum deflection rate, which will prove beneficial to an in-situ creep application where a time to rupture is to be estimated [14]. Moreover, within the last decade, research has demonstrated the capability of the Wilshire equations [15–18] for extrapolation of short term data to predict long life behaviour in a range of alloys, including titanium, copper and steel. These approaches are imperative in understanding the creep deformation process of critical structural components, such as those used in the aerospace industry. One such brand of alloys that undergo aggressive temperature environments whilst in service include single crystal superalloys, materials that are typically used in the high pressure turbine. CMSX-4®[1] is currently the most widely used material for such applications due to the excellent high temperature creep properties that it can offer, particularly when loaded in the [001]-orientation As such, the current work considers results from SP creep tests on CMSX-4 at temperatures ranging from 950 to 1150 °C.

The SP test has traditionally been applied to isotropic materials since the mode of deformation is a biaxial tension state whereby all crystallographic orientations perpendicular to the loaded orientation are deformed simultaneously, thus potentially causing an issue in the application of such a test approach in characterising the creep behaviour of anisotropic materials such as single crystals. Furthermore, previous experimental studies using conventional creep test methods on single crystals have found at intermediate temperatures, in the region of 700 °C; [001] orientated crystals as expected typically exhibit the strongest creep resistance, followed by crystals loaded in the [011] orientation and lastly [111], where the effect is most pronounced during the primary creep phase [19,20]. However, at more elevated temperatures, greater than 980 °C, which is consistent with the temperatures being explored in this research, creep behaviour has been found to be more isotropic than at lower temperatures [19]. For example, at 760 °C with an applied stress of 750 MPa, the creep rupture life of [001] orientated crystals is 1138 h, compared to 36 h in the [111] orientation. On the other hand, at 1050 °C and 120 MPa, [001] orientated crystals exhibit a creep life between 468 and 705 h, [011] orientation a life of 536 h and [111] orientated crystals a life of 474–682 h [19], producing a more isotropic response.

The current research aims to implement a range of lifing techniques to characterise the creep behaviour of CMSX-4, where test data has been gathered from uniaxial and SP creep test approaches. The benefits of such a study may offer significant benefits to the power generation industry, where limited material availability is a typical hindrance in new alloy implementation and the determination of their long term creep life can be a critical issue. Subsequently, the SP creep method is also modelled through ABAQUS to achieve an understanding of the deformation process throughout the SP test when applied to a single crystal material.

## 2. Material and experimental procedure

### 2.1. Single crystal CMSX-4

Fig. 1 shows the microstructure for the second generation nickel based single crystal superalloy CMSX-4, which has a content of approximately 3 wt% Rhenium that significantly improves creep strength. The microstructure consists of a γ matrix, containing a high volume fraction of cuboidal γ′ particles; the interfaces of which are not easily penetrable for dislocations, thus leading to a high creep resistance. The material is cast within 15° of the [001] orientation and following casting the alloy was solution treated at 1312 °C, gas-fan quenched, primary aged at 1150 °C, quenched and finally aged at 870 °C.

[1] ®CMSX-4 is a registered trademark of Cannon-Muskegon Corporation.

### 2.2. Small punch creep test

The small punch creep test is now a widely recognised approach for obtaining useful mechanical property information from limited material availability. Small punch creep tests were performed on a bespoke high temperature SP creep frame developed at Swansea University, as seen in the published literature [10]. In a similar manner to many other established approaches [21], loading was typically applied through the central axis of the rig via an upper load pan arrangement. This load is directly applied to a miniature disc sample through the use of a 2 mm hemispherical ended ceramic punch and the disc is clamped within an upper and lower die, with a 4 mm receiving hole, to prevent any residual flexing motion. The specimen was located centrally within a furnace, and was encased by a ceramic tube to provide an inert argon atmosphere in order to eliminate any potential oxidation effects. To avoid argon leakage, cooling jackets were fitted at either end with PTFE seals to aid retention of frictional contact between the jacket and the tube, and to ensure a hermetic seal for the argon. Deformation was measured through two linear variable displacement transducers (LVDT), one located beneath the load pan which monitors the depth penetration of the indenter, and one located at the underside of the SP specimen via a quartz rod. As such, all of the SP creep tests were performed in accordance with the European code of practice (CoP) [4]. Heat was applied using a digitally controlled furnace and was constantly monitored throughout the test by two Type N thermocouples located in a drilled hole in the upper die, close to the surface of the disc.

Specimen preparation was achieved by turning down cylindrical rods of CMSX-4, that were cast within 15° of the [001] orientation, to 9.5 mm diameter. SP specimens were then prepared by sectioning slices ~800 μm in thickness and ground with progressively finer papers until a 500 ± 5 μm thickness was achieved, in accordance with the CoP [4].

SP and uniaxial constant load creep tests were performed on [001] orientated CMSX-4 specimens over a variety of applied loads and elevated temperatures ranging from 950 °C to 1150 °C.

## 3. Results

Fig. 2 displays the SP creep curves for CMSX-4 tested under an applied load of 190 N across the range of elevated temperatures, showing the SP technique to exhibit what would be considered 'normal' creep deformation, where a decaying primary stage is offset by an accelerating tertiary stage, leading to the observation of a minimum displacement rate, not to be confused with a

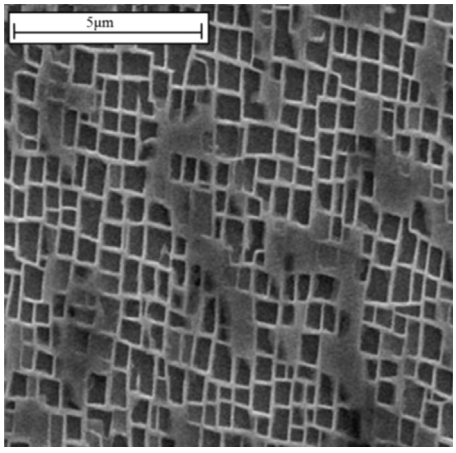


**Fig. 1.** SEM microstructure of CMSX-4.

minimum creep rate, which comes about from a conventional creep test. Fig. 3 shows the SP experimental data generated during the research, illustrating the SP technique as an effective tool for distinguishing sensitivity to both load and temperature for a single crystal material.

From here, the $k_{SP}$ method (Eq. (1)) may then be applied to correlate the SP results to uniaxial creep test data, from which a $k_{SP}$ factor of 0.6 was determined for 950 °C and 0.8 for 1050 °C, as displayed in Fig. 4. The variance in $k_{SP}$ value is attributed the microstructural mechanism of rafting that occurs in single crystal superalloys at temperatures greater than 950 °C. At this temperature rafting may be considered a time dependent process whereas at and above 1050 °C, the phenomenon is thought to occur more rapidly, almost instantaneous [7]. As previously seen [20], CMSX-4, like all other single crystal alloys can evolve from the usual cuboidal γ/γ′ configurations to a plate like microstructure [22], a microstructural transformation that is directly controlled by two factors that occur in the early stages of creep deformation: (i) equilibrium interfacial dislocation networks forming at the γ/γ′ interfaces and (ii) the γ′ particles coalescing by a process of directional coarsening known as the rafting effect [23]. The influence of rafting on creep behaviour was investigated by MacLachlan et al. [24] where they found that depending on conditions of stress and temperature, rafting may have either a detrimental or beneficial effect on creep behaviour. In the early stages of creep deformation, the material response is largely dependent on the extent of microstructural coarsening. However for extended creep lives, the effect of rafting is believed to have a detrimental effect once coarsening has fully developed [23].

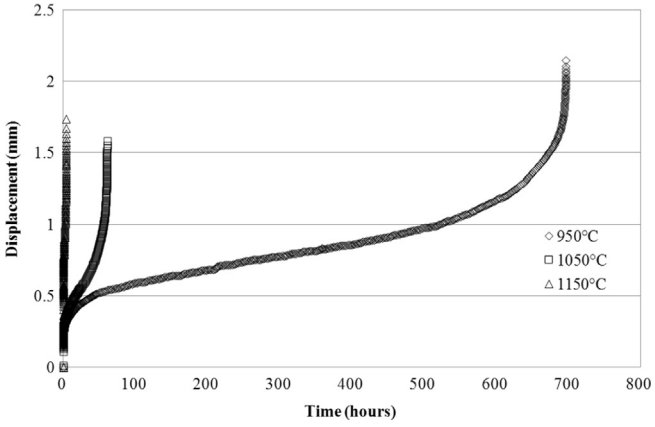


**Fig. 2.** SP creep curves of [001]-orientated CMSX-4 at 190 N over a range of elevated temperatures.

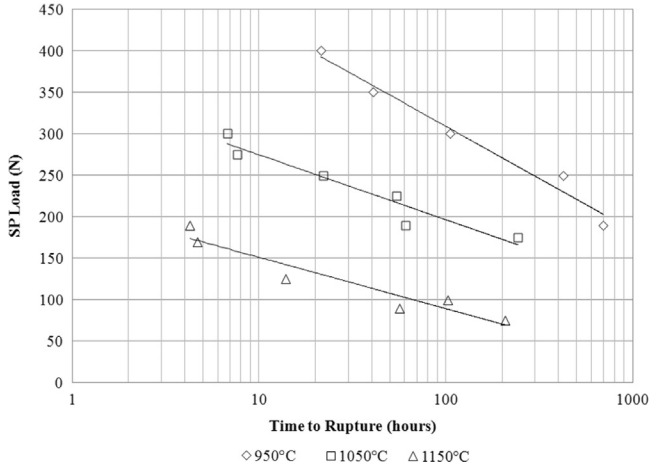


**Fig. 3.** Load vs. time to rupture for CMSX-4 using the SP creep test at a range of elevated temperatures.

## 4. Lifing methodologies and discussion

### 4.1. Monkman–Grant

For the forthcoming empirical correlations, the SP results will be defined in terms of converted SP load into uniaxial stress, that was originally obtained by means of the $k_{SP}$ technique in order to directly compare the different data sets.

In the Small Punch creep test, both time to fracture, $t_f$, and the minimum deflection/displacement rate, $\dot{\delta}_m$, are dependent on the temperature and the acting force [13] with their mutual dependence shown in Fig. 5. These results are compared to uniaxial creep data for CMSX-4 in terms of minimum creep rate, $\dot{\varepsilon}_m$, and time to fracture, $t_f$. Fig. 5 shows the Monkman–Grant relationship for the converted SP data and for the uniaxial creep tests on CMSX-4. This relationship is well documented for uniaxial creep data, as displayed in Eq. (2) and an adapted version for SP data is also given in Eq. (3) [13], where $m_c$, $C_c$, $m_s$ and $C_s$ are constants.

$$\log t_f + m_c \log \dot{\varepsilon}_m = C_c \tag{2}$$

$$\log t_f + m_s \log \dot{\delta}_m = C_s \tag{3}$$

Interestingly, a cross over point is observed at ~0.0015, beyond which the SP data can be seen to fall below the uniaxial results.

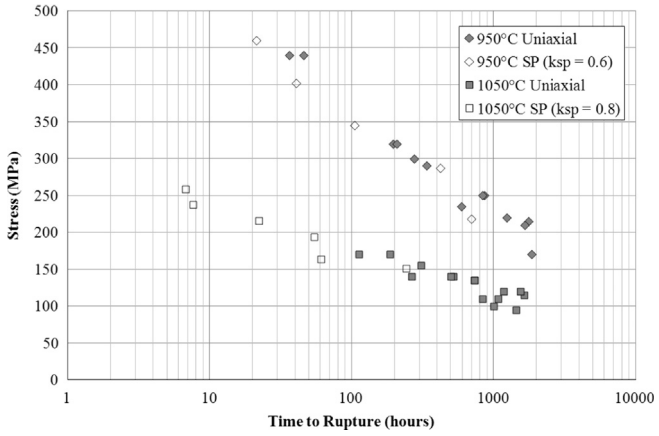


**Fig. 4.** Stress–rupture plot for uniaxial constant load creep tests and converted SP creep data on CMSX-4 at 950 °C and 1050 °C.

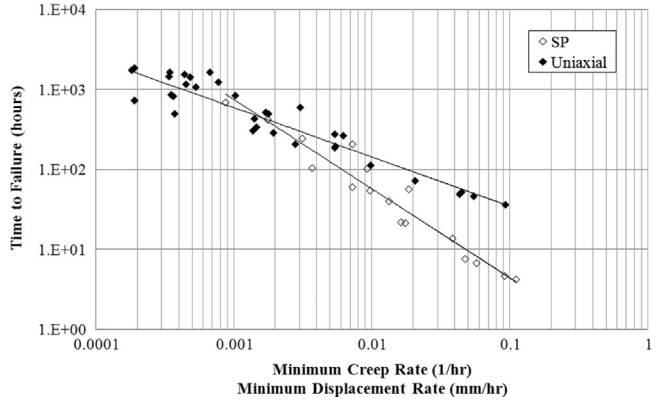


**Fig. 5.** Monkman–Grant relationship for SP and uniaxial creep tests on CMSX-4 at elevated temperatures.

Furthermore, the applicability of using the Monkman–Grant method to correlate the minimum displacement/creep rates is clearly limited as the gradients of the two curves show a distinct difference. Therefore, the contrasting test techniques are difficult to interpret by use of the traditional Monkman–Grant approaches, which is likely attributed to the dissimilar units of minimum creep rate and minimum deflection rate.

### 4.2. Wilshire equations

The Wilshire equations are a modern creep lifing methodology that has previously found success in long life extrapolation of uniaxial creep results. The equations originate from the assumptions that $t_f \rightarrow 0$ as $\sigma \rightarrow \sigma_{TS}$ while $t_f \rightarrow \infty$ as $\sigma \rightarrow 0$. The applied stress, $\sigma$, is shown to be related to the rupture time through the following equation [15]:

$$(\sigma/\sigma_{TS}) = \exp\{-k_1[t_f \exp(-Q_c^*/RT)]^u\} \quad (4)$$

where $t_f$ is the time to rupture in seconds, $\sigma_{TS}$ is the ultimate tensile strength in MPa, $Q_c^*$ is the apparent activation energy for creep in J mol$^{-1}$, $R$ is the gas constant (8.314 J mol$^{-1}$ K$^{-1}$) and $T$ is the temperature in Kelvin. The parameters $Q_c^*$, $k_1$ and $u$ are all derivable from a reasonably comprehensive set of creep rupture data, as is available here from the two test approaches. However, the application of the Wilshire equations has thus far been rather limited to uniaxial creep results. Furthermore, in order to derive the constants necessary to complete Eq. (4) it is first necessary to employ a value for the activation energy, $Q_c^*$. Previous research has shown the activation energy for diffusion in the γ channels to be 290 kJ/mol [25], although dislocation processes have been revealed to be the dominant mechanism in creep deformation [26]. Through plotting $[t_f \exp(-Q_c^*/RT)]$ against $\ln[-\ln(\sigma/\sigma_{TS})]$ the constants $u$ and $k_1$ are easily determined from the gradient and intercept values respectively. Fig. 6 shows the plots for the different test types, where an activation energy value of 145 kJ/mol determines the best fit in each case. This drop in activation energy from that for diffusion in the γ channels could be attributed to preferential diffusion paths at higher temperatures [27], although is considered to more likely due to enhanced freedom of dislocation movement that results from the microstructural coarsening phenomenon of rafting. Wilshire constants are determined as $u=0.1610$, $k_1=0.3049$ and $u=0.1519$, $k_1=0.2259$ for SP creep and uniaxial creep respectively.

Fig. 7 displays the Wilshire prediction in terms of time to rupture as a function of creep stress, for the SP creep data and the uniaxial creep results for [001]-orientated CMSX-4, at 950 °C and 1050 °C. In each scenario, the Wilshire equations offer a close prediction to that of the experimental data, with a better overall match observed at 950 °C. Significantly, at each temperature the Wilshire fits of the SP and uniaxial data sit relativity closely to one another, although the SP Wilshire fit underestimates time to rupture compared to that of the uniaxial. This ability to extrapolate creep failure lives beyond that of the original test data is particularly vital to design engineers since alloys are often placed in applications operating close to the limits of their capabilities, as well as providing useful extended life predictions to the power generation industry, where materials are typically in service for extensive periods of time. Combined with the potential to derive these extrapolations from SP test data, as is presented in this work, the two methods also offer a significant cost saving, as well as further expanding the advantages of both the SP method and Wilshire equations themselves.

### 4.3. Finite element analysis

A numerical model of the SP creep test was developed using ABAQUS 6.13 standard code. Due to the specimen geometry and experimental setup, an axisymmetric model was assumed, where the specimen was firmly clamped along its entire contour. Isotropic material behaviour was also assumed in relation to the findings of previous research [19,20] and 8-node biquadratic axisymmetric quadrilateral elements, with reduced integration (CAX8R) were used. This element type was chosen as it is the most suitable for analysing cases involving large stress and strain gradients, and also in order to accommodate any contact or frictional issues. A model with 810 elements was used for the

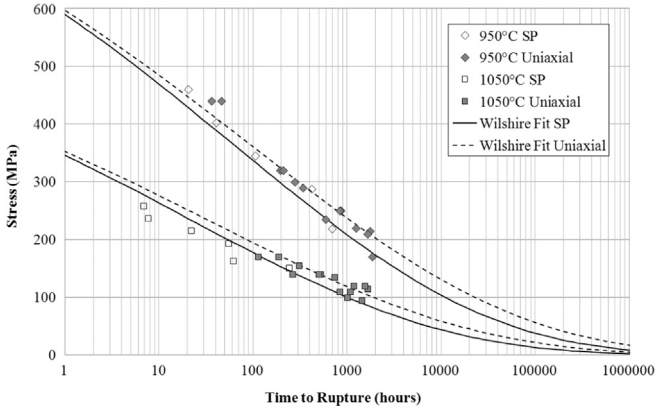


**Fig. 7.** Wilshire equation predictions of time to rupture as a function of stress for CMSX-4 through the SP creep test and the uniaxial creep test.

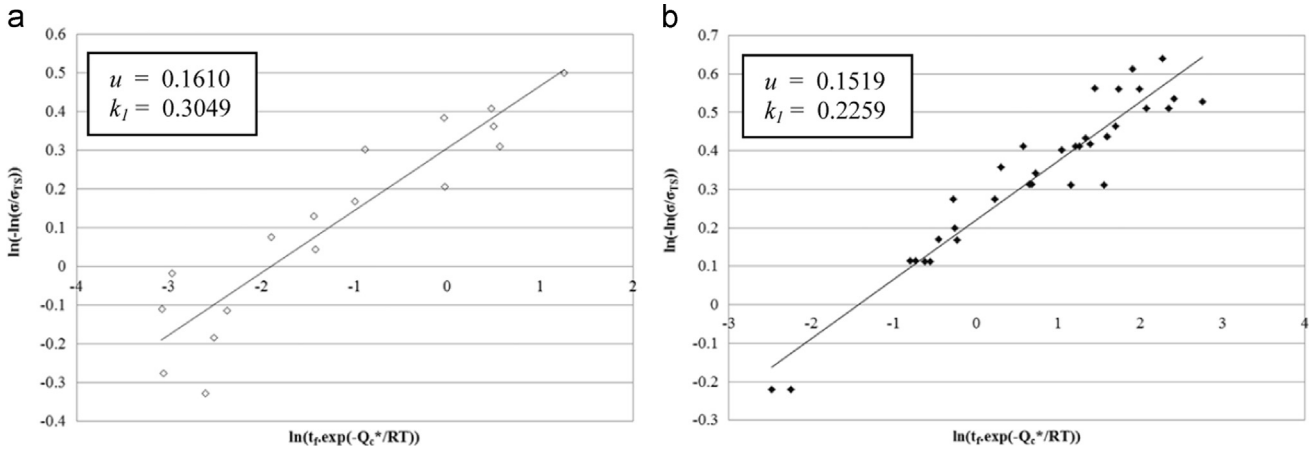


**Fig. 6.** Plot of $[t_f \exp(-Q_c^*/RT)]$ against $\ln[-\ln(\sigma/\sigma_{TS})]$ for $Q_c^* = 145$ kJ mol$^{-1}$ allowing the calculation of $u$ and $k_1$ values for (a) collective SP creep data and (b) collective uniaxial creep data.

0.5 mm thick disc specimen. Following a previous study, the mesh was refined in the region where the highest deformations were expected [28]. The outlay of the mesh employed and the axisymmetric model is shown in Fig. 8, where the specimen thickness is 0.5 mm, specimen diameter is 9.5 mm, the lower die receiving hole is 4 mm, the upper die receiving hole is 6 mm and the punch diameter is 2 mm.

The upper and lower die sets and the punch were modelled as rigid bodies. The friction coefficient was set at $\mu=0.4$, which is a typical frictional coefficient for modelling high temperature contacts, since values from 0.3 to 0.5 reported more realistic results regarding specimen deformation [28,29]. All degrees of freedom of the upper and lower die sets, as well as the horizontal and rotational movement of the punch, were restricted and a vertical load, in the same manner as the experiments, was applied to the punch. For material deformation, a plastic constitutive model was obtained from uniaxial tensile tests as given in Eq. (5), while a power-law creep model was obtained from the uniaxial creep tests (Eq. (6)), where test data is from [001] orientated material. The power-law creep model was preferred for its simplicity and its previous implementation in the ABAQUS code (ABAQUS 6.13), in which it has been proven to produce results of a high quality when modelling the high temperature deformation of various alloy systems [30]. In Eq. (6), $\dot{\bar{\varepsilon}}^{cr}$ is the uniaxial equivalent creep strain rate, $\tilde{q}$ is the uniaxial equivalent deviatoric stress, $t$ is the total time and $A$, $n$ and $m$ were obtained from experimental uniaxial creep data following the methodology described by Maximov et al. [30]. Furthermore, previous research has shown that for feasible correlations, $A$ and $n$ are to be positive and $-1<m\leq 0$ [30]. For these simulations a damage model was not implemented, so it was assumed that the numerical model is only valid until crack/necking initiation. Furthermore, the effect of elastic anisotropy has not been incorporated into the model.

$$\sigma = K\cdot {\varepsilon_p}^N \tag{5}$$

$$\dot{\bar{\varepsilon}}^{cr} = A\cdot \tilde{q}^n \cdot t^m \tag{6}$$

The parameters obtained for each material model are given in Table 1

Fig. 9 shows a comparison of the time–displacement behaviour for a series of SP creep tests and the curves generated through the

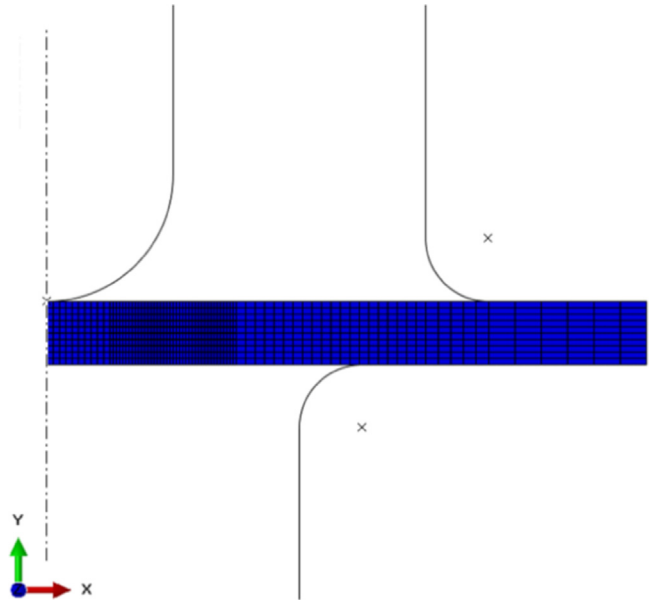


**Fig. 8.** Axisymmetric model geometry and mesh employed using ABAQUS.

**Table 1**
Parameters used for the material models.

| Temperature (°C) | E (GPa) | ν | K | N | A ($MPa^{-n}h^{-m-1}$) | n | m |
|---|---|---|---|---|---|---|---|
| 950 | 88.1 | 0.415 | 981 | 0.027 | $8.06\times10^{-13}$ | 4.21 | −0.40 |
| 1050 | 79.9 | 0.425 | 633 | 0.067 | $9.00\times10^{-8}$ | 2.13 | −0.20 |

ABAQUS modelling simulation software. Upon initial inspection the correlation between the experimental and ABAQUS results appear better at 950 °C than at 1050 °C, particularly in the 'primary' phase of the creep response, although a reasonable conformity is still seen in the latter. It is believed these differences may be attributed to the ambiguous effects of rafting on creep response, which the simulation will not account for. When creep life is expected to be long, under low stresses, rafting is thought to be detrimental, however, rafting is considered partially responsible for the creep-hardening effect that takes place during the initial phase of creep [23]. This creep hardening effect is expected to be prominent in the 1050 °C experimental data, since previous research has shown the rafting phenomenon to be a time dependent process at 950 °C and a temperature dependent process at 1050 °C, in that it occurs almost instantly [7]. Nevertheless, it is perhaps the point of minimum displacement, at which a comparison can be made that offers a better insight into the application and advantages of such a model. In order for a practical comparison to be made, the time at which the minimum displacement rate occurs in the experimental data is used as the time at which minimum displacement rate is recorded in the numerical simulations. These minimum displacement rates are compared in Fig. 10, further highlighting that the simulations at 950 °C tend to be in better agreement with the experimental results than at 1050 °C.

To accompany the experimental vs. numerical SP creep plots, an analysis of the 'thinning' phenomenon that occurs at the centreline of the specimen has also been assessed. To understand this, an SP test performed at 1050 °C under a load of 190 N, was interrupted after a period of 53 h, by which point a displacement of 0.65 mm had been achieved. The miniature disc specimen was then sectioned through the centreline to measure the degree of specimen thinning, or how much the cross section of the disc had reduced, as indicated in Fig. 11. The same process was then followed for the numerical modelling, whereby a simulation was interrupted after 0.65 mm of displacement and the extent of thinning was measured at the centreline. As shown in Fig. 11, a very good agreement is seen between the two, with a cross sectional thickness of 428 μm measured in the experimental sample, and a thickness of 423 μm was observed in the numerical simulation. A full comparison is given in Table 2.

## 5. Conclusions

A series of lifing approaches, in particular the Wilshire equations and finite element modelling, have been applied to CMSX-4 test results, where the experimental data was obtained by both the small punch and uniaxial creep testing techniques. The following conclusions can be made:

- The Wilshire fits have been proven to correlate well in both the SP and uniaxial creep test methods across the two experimental temperatures, 950 °C and 1050 °C for CMSX-4.
- The value for apparent activation energy derived through the Wilshire equations is found to be the same for both test techniques ($Q_c^*=145$ kJ mol$^{-1}$), which is less than that quoted for diffusion in the γ channels, understood to be due to the

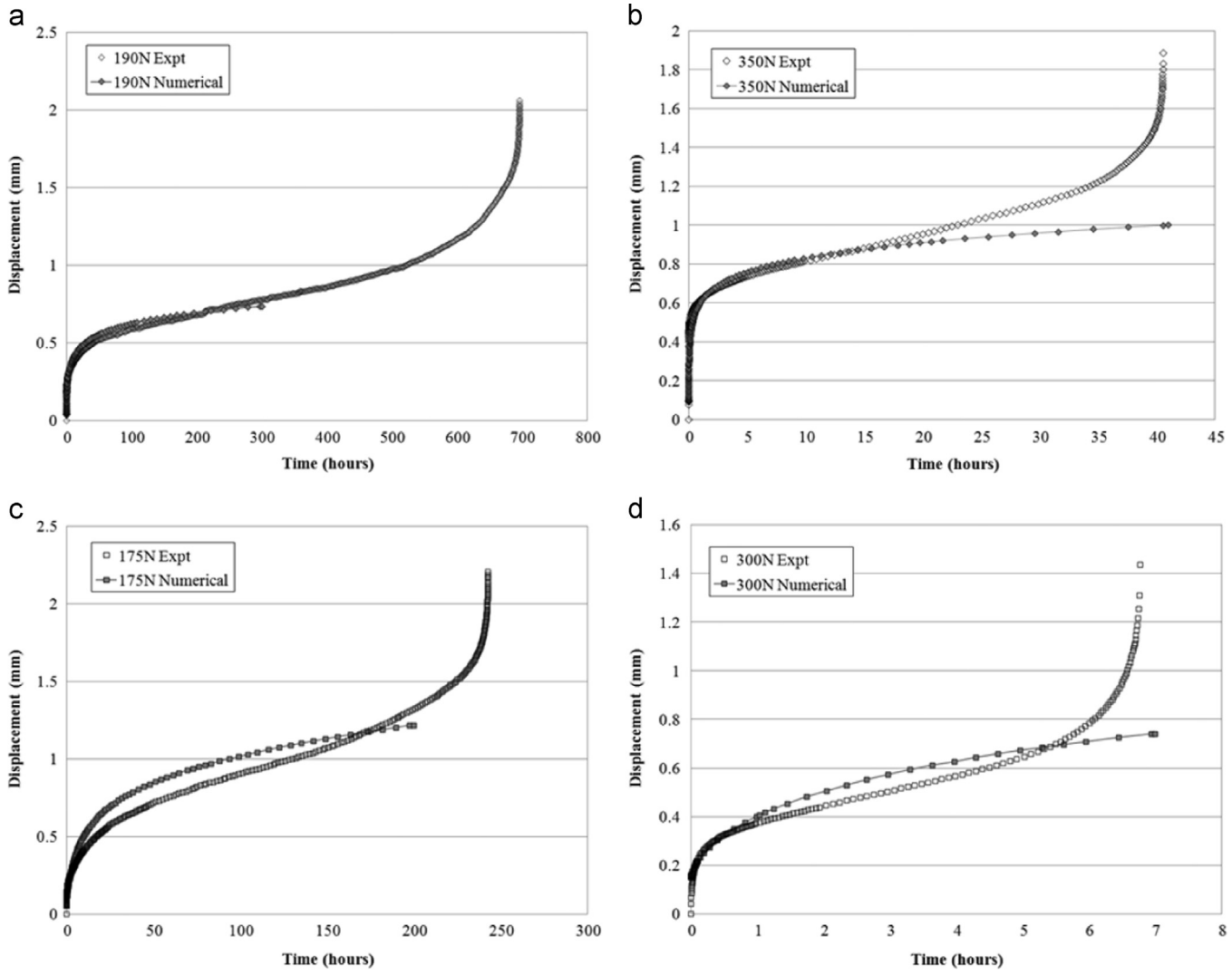


**Fig. 9.** Comparison of the experimental results with the numerical simulations in ABAQUS. (a) 950 °C and 190 N; (b) 950 °C and 350 N; (c) 1050 °C and 175 N; (d) 1050 °C and 300 N.

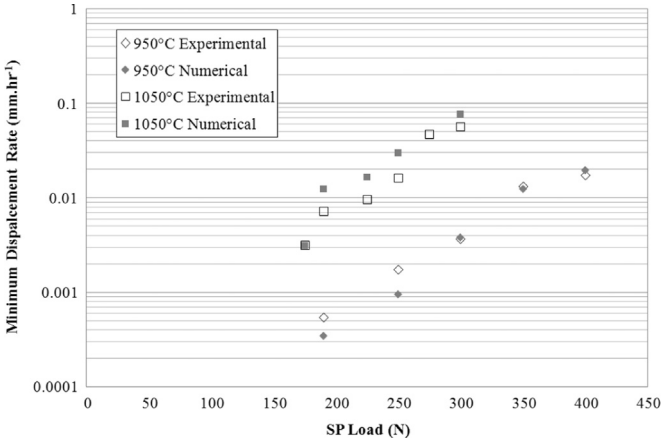


**Fig. 10.** Comparison of minimum displacement rates obtained in the experimental results and the numerical simulations in ABAQUS.

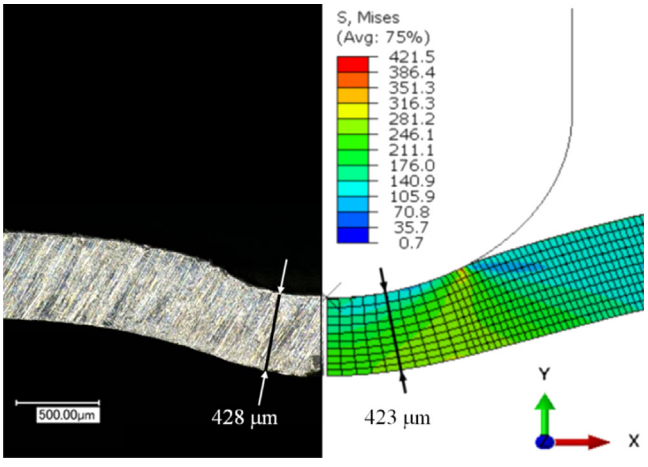


**Fig. 11.** Interrupted SP creep test at 1050 °C with a 190 N loading showing thinning at the centre of the specimen (left: experimental, right: numerical).

creep deformation being dominated by dislocation processes and the microstructural coarsening known as the rafting regime that takes place at these elevated temperatures.

- A good agreement is observed between the ABAQUS SP simulations, completed using uniaxial data, and experimental SP creep response at both 950 °C and 1050 °C, particularly when calculating minimum displacement rates.

**Table 2**
Miniature disc thinning measurements.

| | Load (N) | Displacement (mm) | Time (h) | Centre (μm) |
|---|---|---|---|---|
| Experimental | 190 | 0.65 | 53 | 428 |
| Model to fixed displacement | 190 | 0.65 | 17 | 423 |

- The drop in the early stages of the experimental creep response compared to the simulations at 1050 °C is attributed to the rapid onset of rafting at this temperature, and the resulting creep hardening effect.

## Acknowledgements

The current research was funded under the EPSRC Rolls-Royce Strategic Partnership in Structural Metallic Systems for Gas Turbines (Grants EP/H500383/1 and EP/H022309/1). The provision of materials and technical support from Dr. Neil Jones and Dr. Duncan MacLachlan at Rolls-Royce plc. are gratefully acknowledged. The authors would also like to thank Dr. Mark Whittaker for their help and advice in preparation of the manuscript.

## References

[1] M.P. Manahan, A.S. Argon, O.K. Harling, J. Nucl. Mater. 104 (1981) 1545–1550.
[2] F. Di Persio, G.C. Stratford, R.C. Hurst, in: J. Veivo ,P. Auerkari (Eds.), Baltica vi: life management and maintenance for power plants, vol. 1–2, 2004, pp. 523–535.
[3] D. Norris, J.D. Parker, Mater. Sci. Technol. 12 (1996) 163–170.
[4] CEN Workshop Agreement CWA 15267, European Code of Practise: Small Punch Test Method for Metallic Materials, 2007.
[5] V. Bicego, F. Di Persio, R.C. Hurst, G.C. Stratford, Comparibility of results via the miniaturised small punch test method and traditional uniaxial creep testing, in: Proceedings of 11th International Conference on Fracture, 2005, pp. 4808–4814.
[6] E.C. Moreno-Valle, W. Pachla, M. Kulczyk, B. Savoini, M.A. Monge, C. Ballesteros, I. Sabirov, Mater. Sci. Eng. A 588 (2013) 7–13.
[7] S.P. Jeffs, R.J. Lancaster, Mater. Sci. Eng. A (2014).
[8] V. Bicego, J.H. Rantala, J. Klaput, G.C. Stratford, F. Di Persio, R.C. Hurst, The small punch test method: results from a European creep testing round robin, in: Proceedings of 4th International Conferences in Advances in Materials Technology for Fossil Power Plants, 2004.
[9] R.J. Lancaster, R. Banik, R.C. Hurst, M.R. Bache, Application of small punch test methods to advanced manufactured structures, in: Proceedings of the 3rd International Conference Small Scale Test Techniques 2014, 2014, pp. 170–178.
[10] R.J. Lancaster, R.C. Hurst, G. Norton, M.R. Bache, J. Lindemann, Small punch creep testing of next generation TiAl alloys, in: Proceedings of 3rd International European Creep Collaborative Committee on Creep and Fracture, 2014.
[11] K. Turba, R.C. Hurst, P. Hähner, J. Nucl. Mater. 428 (1–3) (2012) 76–81.
[12] D.C. Dunand, B.Q. Han, A.M. Jansen, Metall. Mater. Trans. A 30 (13) (1999) 829–838.
[13] F. Dobeš, K. Milic, Mater. Sci. Eng. A 336 (2002) 245–248.
[14] J.M. Alegre, I.I. Cuesta, M. Lorenzo, Exp. Mech. 54 (8) (2014) 1441–1451.
[15] B. Wilshire, A.J. Battenbough, Mater. Sci. Eng. A 443 (1–2) (2007) 156–166.
[16] B. Wilshire, P.J. Scharning, Scr. Mater. 56 (12) (2007) 1023–1026.
[17] B. Wilshire, P.J. Scharning, Scr. Mater. 56 (8) (2007) 701–704.
[18] M.T. Whittaker, W.J. Harrison, R.J. Lancaster, S. Williams, Mater. Sci. Eng. A 577 (2013) 114–119.
[19] P. Caron, Y. Ohta, Y.G. Nakagawa, T. Khan, Sixth International Symposium on Superalloys, Superalloys (1988) 215–224.
[20] C. Knobloch, S. Volker, D. Sieborger, U. Glatzel, Mater. Sci. Eng. A 234-236 (1997) 237–241.
[21] T.E. García, C. Rodríguez, F.J. Belzunce, C. Suárez, J. Alloy. Compd. 582 (2014) 708–717.
[22] A. Royer, P. Bastie, M. Veron, Acta Mater. 46 (15) (1998) 5357–5368.
[23] R.C. Reed, The Superalloys: Fundamentals and Applications, Cambridge University Press, USA (2006) 180–186.
[24] D.W. MacLachlan, D.M. Knowles, Mater. Sci. Eng. A 302 (2) (2001) 275–285.
[25] J. Svoboda, P. Lukis, Mater. Sci. Eng. A 234–236 (1997) 173–176.
[26] M.T. Whittaker, B. Wilshire, Metall. Mater. Trans. A 44 (S1) (2012) 136–153.
[27] R.W. Evans, B. Wilshire, Introduction to Creep, The Institute of Materials, Swansea (1993) 30.
[28] J.P. Rouse, F. Cortellino, W. Sun, T.H. Hyde, J. Shingledecker, Mater. Sci. Technol. 29 (11) (2013) 1328–1345.
[29] P. Dymáček, K. Milička, Mater. Sci. Eng. A 510–511 (2009) 444–449.
[30] J.T. Maximov, G.V. Duncheva, A.P. Anchev, M.D. Ichkova, Comput. Mater. Sci. 83 (2014) 381–393.